Research Square

Preprints are preliminary reports that have not undergone peer review. They should not be considered conclusive, used to inform clinical practice, or referenced by the media as validated information.

Study on Mechanical Property and Biocompatibility in Vitro of 3D Printing Tantalum- Niobium Alloy Implants.

Huiling Li
Central South University Xiangya School of Medicine https://orcid.org/0000-0003-2777-990X

Jian Zhang
Z-BEST Dental Science and Technology CO.LTD, Hunan.

Zhigang Yao
Central South University

Junhui Huang (huangjunhuixy@163.com)
Central South University Xiangya School of Medicine

Research

Keywords: 3D-printing, SLS, Tantalum-Niobium alloy, implant, human Oral Mucosa Fibroblast, mechanical property, biocompatibility

Posted Date: February 26th, 2021

DOI: https://doi.org/10.21203/rs.3.rs-249911/v1

License: This work is licensed under a Creative Commons Attribution 4.0 International License. Read Full License

---

Abstract

tooth defects or deletions. Tantalum (Ta) has been widely used in the biomedical field, but its application in artificial dental implants is rarely reported. In this study, Tantalum-Niobium alloy (TaNb40) implant prepared by 3D printing—SLS was used as the research subject. Its mechanical properties in vitro and the biocompatibility by utilizing human Oral Mucosa Fibroblasts (hOMF) were studied.

Results: The mechanical property test results were that the Tensile Strength, Yield Strength, Elongation, and Vickers hardness of TaNb40 implant was 548 ± 50MPa, 420 ± 30MPa, 40%, and 425HV, respectively, manifesting the two indicators met the requirements of dental metal implant, and had good mechanical properties of wear resistance and not easy to brittle fracture. The cytocompatibility test showed that TaNb40 did not inhibit cell proliferation and produce cell cycle arrest. The cytotoxicity grade was 1, there was almost no metal ion release in the culture medium, and the surface had fine cell early adhesion, which met the requirements of biomedical materials.

Conclusion: The TaNb40 prepared by domestic 3D printing—SLS has excellent mechanical properties and cytocompatibility in vitro, which is expected to replace the Titanium metal implant prepared by the traditional casting method, having a leading significance for the formation of implants with independent intellectual property rights.

Background

The development of medicine and materials science largely depends on people's continuous pursuit of life quality and life expectancy. The defects or deletions of certain tissues or organs are caused by some diseases, trauma, and other factors. To restore their morphology and physiological function, biomedical materials are needed to repair the damaged tissues. Among them, bio-metallic materials are good substitutes for the defects in the body, which have high mechanical strength, stable chemical properties, and excellent biocompatibility. At present, metal materials are mainly used in artificial joints, internal fixation of trauma, spine and orthopedic restoration, etc. Three widely used biomaterials in orthopedics include Stainless Steel (SS), Cobalt-based alloy, and Titanium (Ti) alloy [1]. According to the number and type of dentition defects or deletions, different prosthodontics can be adopted, including fixed denture, removable denture, and implant restoration. Implant restoration, a permanent structure, is an important way to replace the missing teeth, the system mainly consists of two parts: implant and abutment. The abutment is fastened to the implant by a screw, and provides a fixed point for tooth restoration [2]. Therefore, it not only has the advantages of good retention, stability, high masticatory efficiency, and no damage to other teeth but also beautiful appearance and comfort, which has become a popular repair method for clinicians and patients. The abutments can be made of different materials, including Ti, Gold, Zirconia, Alumina, and polymer [3]. In the late 1960s, the first batch of ceramic dental implants made of Alumina was developed, however, due to its poor mechanical properties, it was easy to fracture when loaded with external force, and finally was driven out of the market [4-5]. At present, most dental implants are composed of commercially pure Ti, which is a highly biocompatible material with a survival rate of

90.9% to 97.7% after 15 years of implantation [6-8]. The high success rate is partly owing to the formation of oxide film (mainly TiO2), which separates the base metal from the tissue and provides a suitable surface for osseointegration [9]. Although the excellent performance of Ti implants is attributed to surface properties to some extent, the mechanical properties may not be sufficient in applications requiring narrow diameter, short implants, or exposure to excessive occlusal stress [10]. Therefore, for the sake of improving the osseointegration and long-term survival rate of implants, many researchers focus on the development of multifunctional Ti surfaces. For example, in addition to sandblasting and acid-etched surfaces, there are some scientific reports on the survival rates of the Branemark dental implant system (anodized TiO2 surface) and Astra Tech dental implant system (TiO2 surface / sandblasting), and the biological activity of Ti is improved by adding bioactive microelement [11-12]. In recent years, Titanium-Zirconium (TiZr) alloy and Zirconia (ZrO2) have become alternative materials due to their high mechanical strength and low corrosion sensitivity [13]. TiZr alloy is a promising candidate material, which can also reduce the cytotoxicity related to Ti alloy other components, especially Aluminum (Al) and Vanadium (V) [14-15]. The natural oxide film of Zr increases its passivation, compared with pure Ti, the release of metal ions is significantly reduced when immersed in acid medium of the simulated oral environment [16]. Although TiZr alloy has improved its corrosion resistance, it is similar to Ti substrate in terms of initial bacterial attachment and biofilm formation [17]. Like Ti, ZrO2 also presents an oxide surface, which is conducive to bone integration similar to Ti [18-19]. However, accelerated aging in the water environment will lead to partially stable ZrO2 oxide film degradation[20-21]. Because the success rate of implant implantation is related to many factors, such as bone quality, implant interface properties, stress distribution around the implant, so the research and development of new implant materials need to make up for the deficiencies of the current materials in terms of biomechanical properties. Moreover, as we all know, China has a large population, the dental implants and other high-quality materials mainly rely on imports. Besides, there are some metal and alloy dental implant materials in the Chinese market, existing different degrees of histocompatibility and toxic side effects of alloy elements on the human body, as well as, the variety is single, and the price is expensive. One of the key goals of life science in China's medium and long-term science and technology development plan is to develop new-type biomedical materials such as individualized medical engineering technology and human tissue organ replacement.

Tantalum (Ta) is a transition group element, which belongs to the VB group in the periodic table. Its melting point is as high as 2995 ℃, Ta alloy has excellent thermal shock resistance and molding toughness. Besides, it also has high thermal and electrical conductivity. Therefore, Ta is widely used in electronics, chemical industry, aviation, weapon system and other aspects [22-24]. In the air and other media, the Ta surface layer will react with oxygen or other oxidants to form an oxide film, which has a more compact structure and insulation performance, and excellent corrosion resistance [23]. As early as the middle of the 19th century, the biomedical field began to use this metal to prepare pacemaker electrode materials, nerve repair films, and head modeling versions, etc [25]. Stable biological characteristics make Ta play an important role in the medical field, such as Ta nail for the treatment of early adult femoral head necrosis, Ta metal rod supporting bone tissue defect, the trabecular metal used

in joint and spinal surgery, etc. [26-29]. At present, Porous Tantalum Trabecular Metal (PTTM) has been incorporated into Ti alloy dental implants to improve osseointegration in many studies, but Ta as an artificial root is rarely reported. Solid pure Ta has high mechanical strength and density (16.68g/cm3), therefore, porous structure involving porosity and pore diameter has obvious advantages in this aspect. By adjusting the porosity and pore size of the material, the "stress shielding" is reduced or eliminated, so that facilitating its elastic modulus to match that of human bone tissue. However, high melting temperature, a strong affinity for oxygen, difficulty in material preparation, and high cost make it very difficult to prepare Ta through ordinary methods, which limits the wide application of Ta [30]. Ta and Niobium (Nb) are geared to the same category in the periodic table of elements. Nb has a lower melting temperature (2477℃), elastic modulus, and raw material cost than Ta and Nb is a strong β stabilizer [30-31]. Therefore, the Ta-Nb alloy has a lower elastic modulus than the Ta scaffold, without inhibiting its corrosion resistance or introducing any cytotoxic components, and reducing the manufacturing cost.

3D printing is a highly adjustable and complex device matching with human anatomy position, which is suitable for patients and has become a leading manufacturing technology in the field of health care and medicine [32]. 3D printing, also known as additive manufacturing or additive rapid prototyping, can rapidly and accurately manufacture 3D stacked objects of complex shape under the control of the computer through the precise design of models [33]. At present, Stereolithography (SLA), Fused Deposition Modeling (FDM), Selective Laser Sintering (SLS), and Three-dimensional printing (3DP) are common methods in 3D printing [34]. Among them, SLS is a kind of technology that makes use of powder and computer-control to rapidly separate and produce objects. It uses a laser to combine powder particles, building them layer by layer, and then gain them from under the powder bed [35-36]. Compared with FDM, SLS is a single-step process that does not require hot-melt extrusion to pre-produce suitable filaments and produces higher resolution ratio objects due to laser accuracy [37-39]. 3D printing is gradually rising in medicine. Brito [40] reported the advantages of additive manufacturing in mandibular fracture surgery. Mafeld [41] carried out the feasibility study of the 3D printing vascular model. Ren [42] used 3D printing to design a calcaneal surgical guide plates to improve the surgical treatment scheme. Tetsworth [43] applied 3D printing to the reconstruction of complex post-traumatic osteoplasty and achieved ideal results. Personalized biomedical materials can be prepared by 3D printing to meet the needs of different patients. It has broad prospects in terms of tissue scaffold, cell printing, prosthesis. The 3D printing in the research and development of biomaterials involves the following key technologies: firstly, digital three-dimensional Computer-Aided Design (medical prototype object simulation) system(CAD), which transforms CAD model into "clone" products of real tissues or organs; secondly, medical biomaterials with 3D printing; thirdly, the technology and equipment suitable for biomedical materials printing. These are indispensable.

Although 3D printing has gained the attention of many domestic and foreign scholars, especially in the preparation of biomedical materials, the clinical application of 3D printing still faces many challenges, which are still in the initial stage. The first problem is CAD software and the selection of 3D printing raw materials including the mechanical properties, biocompatibility and activity retention, etc. Secondly, if 3D printing is applied to living cells or tissues, the survival rate of cells on the surface or inside of the product

needs to be maintained during the whole processing. Finally, we need to clarify the mechanism of cell adhesion, growth, and differentiation inside the material.

To develop new-type material implants with independent intellectual property rights, reduce or eliminate the dependence on imports, and provide Chinese with suitable prices, multiple choices, and better performance implants, Ta-Nb alloy implant taking Ta as the main component and adding the appropriate amount of Nb was prepared by domestic 3D printing equipment and SLS technology in the early stage. In this study, a traditional Ti implant was used as a control. The main research contents include the Tensile Strength(TS) and Hardness analysis in vitro of Ta-Nb alloy implant. Effects of Ta-Nb alloy on the growth, proliferation, migration, early adhesion, and cell cycle of human Oral Mucosa Fibroblasts(hOMF). The content of metal ions in the different extracting liquid was analyzed to determine the stability of metal materials. The research of this project is of great theoretical and practical significance to improve China's independent innovation ability, promote the development of the 3D printing industry chain and prosthodontics.

Results

General observation of experimental materials

Tantalum-Niobium alloy (TaNb40) implant material was prepared by SLS. SLS laser parameters were 250W. Its size is 4.5mm in diameter, height 12.2mm, and weight 2.2g (without abutment). The shape is similar to that of Ti implant commonly used in the clinic (Fig. 1 and Fig. 2). It can be seen from Fig. 1 that the surface of the TaNb40 alloy is bright gray with a certain degree of roughness, which is the original shape that has not been surface treated. To facilitate the co-culture of experimental materials and cells, and the TaNb40 alloy disc prepared by SLS was used to replace the implant for an experiment in vitro. The surface of the substitute was bright silver (Fig. 3). There is little difference in appearance between Ta, Ti, and Ni metal samples prepared by the traditional casting method (Fig. 4).

The mechanical properties of TaNb40 implant

TaNb40 implant was tested by a Third-Party Inspection Agency and placed on a tensile tester to detect the tensile property of the material, including TS (Mpa), Yield Strength (YS) (Mpa), and Elongation (%), a routine test item of metal material. The results were shown in Table 1. The TS, YS, and Elongation of TaNb40 implant were 548 ± 50MPa, 420 ± 30MPa, and 40%, respectively, besides, the Vickers hardness was 425HV.

Growth of Cells

The morphology of primary hOMF cultured to the 5th-6th generation is shown in Fig. 5, observed cell morphology after recovery was brightly circled under an inverted microscope, and cells had well-defined nuclear membranes. After 24 hours [Fig .5(a1)-(a3)], most of the cells emerged long fusiform, a few cells had more branches, extended outward, and it changes like starlike. On the 3rd day [Fig.5(b1)-(b3)], the

cells grew rapidly, increased number, the processes connected. On the 5th-7th day [Fig. 5(c1)-(c3) and Fig.5(d1)-(d3)], the cell volume increased, and the processes fused into a network, increased cell density and collagen matrix secretion could be observed clearly after HE staining. In this experiment, the 5th-6th generation cells as samples grew well, whose morphology was consistent with that of normal fibroblasts.

Direct effects of materials on cells

As shown in Fig.6, compared with the normal control in Fig.5, the number and morphology of cells of the co-culture with TaNb40, Ta, Ti, and Ni on the 1st, 3rd and 5th day were as follows: (1) On the 1st day[Fig.6(a1)-(d1) and Fig.6(a2)-(d2)], the cells in the experimental group (TaNb40, Ta) and the positive control group (Ti) grew well, a very few non-adherent cells were observed. There was little difference in cell morphology among the three groups under the light microscope. However, only about 50% of the cells adhered to the wall in the negative control group (Ni), the adherent cells were not in good shape, showing the short rod-shaped structure and no polygonal cells. (2) On the 3rd day[Fig.6(a3)-(d3) and Fig.6(a4)-(d4)], the number of cells gradually increased, the processes were connected into reticular formation in the TaNb40, Ta, and Ti group. On the 5th day[Fig.6(a5)-(d5) and Fig.6(a6)-(d6)], the cells in TaNb40 and Ta groups were densely distributed around the materials, and a small amount of cell apoptotic fragments was observed. There was no cell attachment in the area about 0.1 mm around the Ti sheet, and the cells outside this region grew and arranged well. According to the cytotoxicity scoring standard in vitro, the score of these three materials can be recorded as 0. In the Ni group, about 80% of the cells were round with no protruding pseudopodia, the number of cells decreased as the dissolution of some cells, and the above morphological changes became more obvious over time, there were almost no normal adherent cells on the 5th day, the cytotoxicity was grade 4, which was material with severe cytotoxicity. (3) The cells at different distances from the same material on the same day showed that there was no significant difference between TaNb40 and Ta at three-time points, but the number of cells far away from Ti seemed to be slightly more than that around the material. In the Ni group, it seems that the cells farther away from the material were in better condition at the same time than those near the material.

Effects of materials on cell early adhesion

The micrographs of adherent cells after AO fluorescence staining were shown in Fig.7. In the TaNb40 and Ta group, the cell showed a large amount of clear green fluorescence, which was evenly distributed on the surface of the material, and the number of adhesion cells increased significantly with time. In the Ti group, most showed red and yellow fluorescence, which represented the difference of binding capacity between staining agent and DNA. The cells were scattered in different visual fields, and a small number of cell fragments and apoptotic bodies could be seen, the amount at the 12th hour was significantly more than that at the 4th and 6th hour. In the Ni group, the quantity was significantly less than that of the other three groups at each time point. It can be seen that the chromatin shrinks and breaks into patches of varying sizes, showing the shape of green fragments, and only a few cells adhered at three-time points.

According to the quantitative analysis in Table 2 and Fig.8, the comparison of cell adhesion rate was successively Ti > Ta > TaNb40 > Ni and the difference between Ti and Ta, Ti and TaNb40 was statistically significant ($P < 0.05$). At the 6th and 12th hour, the cell adhesion rate successively was Ta > TaNb40 > Ti > Ni, there were significant differences between Ta and Ti, TaNb40 and Ti ($P < 0.01$). The adhesion rate increased with time in TaNb40, Ta and Ti group, and the highest at the 12th hour. No significant difference between the 4th and 6th hour in the Ti group ($P > 0.05$), but it increased significantly between the 6th and 12th hour ($P < 0.01$). However, The adhesion rate of the Ni group was very low at all time points, and the mean value of the TaNb40 and Ta group exceeded 100% at the 12th hour. It can be seen that both TaNb40 and Ta have no effect on cell adhesion, and the initial adhesion process of surface cells was even better than that of Ti, and can quickly adhere to the surface in the early stage.

Effects of materials on cell proliferation

To evaluate the effect of different material extracting liquid on cell proliferation, using CCK-8 reagent and enzyme labeling to detection. According to the quantitative analysis results in Fig.9, on the 1st day, the cell proliferation activity (OD value) was as follows: blank control > Ta > Ti > TaNb40 > Ni, Ta and Ti group ($P < 0.05$), TaNb40 and Ti group ($P < 0.01$). On the 3rd day, the comparison was blank control > Ta > Ti > TaNb40 > Ni, there was statistical difference between Ti and Ta Group ($P < 0.05$), but there is not between Ti and TaNb40 group ($P > 0.05$). On the 5th day, the order successively was blank control group > Ti > Ta > TaNb40 > Ni, Ti and TaNb40 group ($P < 0.01$), Ti and Ta Group ($P > 0.05$). The OD value of the blank control group at each time point showed the highest cell activity ($P < 0.01$). There was no statistical difference in the OD value of the Ni group at three-time points. As can be seen from Fig.9, the number of cells did not increase but also decreased with time.

The RGR and cytotoxicity grade as shown in Table 3 were calculated from the OD value. The Ta, TaNb40, and Ti group was grade 1, which met the requirements of medical biomaterials, while the Ni group was grade 3, which did not conform to the specification of medical biomaterials.

Effects of materials on cell cycle

As shown in Fig.10, the cell cycle distribution was detected by flow cytometry after 48 hours of treatment with different extracting liquid, and the data were listed in Table 4. The one-way ANOVA analysis on the percentage of cells in G1, G2, and S phase among the five groups in Table 4 indicated there were significant differences among the phase of each cycle between groups($P < 0.01$). However, compared with the blank control group, the percentage of G1 / S phase cells tended to increase and the G2 phase decreased in the Ta Group. The TaNb40 group increased in the G1 phase and decreased in S / G2 phase, although the cell cycle percentage of the TaNb40 group was statistically different compared with a blank control group, it tended to be similar in numerical value, and there was no significant increase or decrease. In the Ti group, the G1 phase decreased and S / G2 phase increased. In the Ni group, the percentage of S-phase cells increased significantly, and Ni induced S phase arrest accompanied by a

decrease in the percentage of G1 phase cells. Compared with 3.11% of the blank control group, the cells treated with Ni had the highest apoptosis percentage of 3.91% in the sub-G1 phase.

Detection of metal ion content

The content of metal ions in the four kinds of material extracting liquid was listed in Table 5. The amount of ions released by Ni was the highest, up to 264 mg/kg. The metal ions were hardly detected in other groups. In the reference data of detection limit value, the amount of the ions of TaNb40 and Ta Group were less than 0.1mg/kg, and that of Ti group were less than 0.2mg/kg.

Discussion

At present, Ta is widely used in the biomedical field, especially in orthopedic metal implants, which attracts the attention of researchers in the field of biomaterials. In recent years, PTTM has been incorporated into Ti alloy dental implants to improve osseointegration. Compared with traditional bone implant materials, Ta has high corrosion resistance, hardness, and wear resistance, which can avoid the adverse biological effects to the most extent caused by the release of metal ions in vivo. On the other hand, Ta has strong osteoinductive and osseointegration abilities in vivo, even better than Ti dental implants, which can improve the stability of implants at the early stage [44-46]. However, Ta is a relatively active element, the powder particle size is small, and it is easy to oxidize at high temperature, so it is difficult to prepare, at the same time, the mechanical strength and density of solid pure Ta are very high. Adding Nb element can improve the mechanical properties of the material, reduce the sintering temperature and manufacturing cost, and promote the sintering of Ta at high temperature, to meet the clinical requirements of dental implant material. Also, the traditional processing technology is difficult to prepare Ta, therefore, SLS was used to meet the personalized requirements in the early stage of this study. The surface of TaNb40 alloy prepared by SLS is brightly gray with a certain roughness, moreover, the oxygen content is lower than 40ppm in the degreasing environment, and there is no oxidation phenomenon. As a load-bearing part of the body, the bio-metal orthopedic implant must have good mechanical properties. In addition to evaluating the stability of implant through bone integration, the matched mechanical properties between the alloy and bone tissue are conducive to the uniform distribution of force transmission to the alloy and surrounding bone tissue, and prevent the generation of "stress shielding" [47]. Mechanical properties and biocompatibility are the primary factors to be considered in the design of new materials [48]. Especially in the dental implant, they will be exposed to the alternating stress of load and fatigue when performing their functions [49]. The strength of the alloy shall be high enough to withstand external forces including tension, compression, bending and torsion [48, 50]. TS and YS are the basic properties of hard tissue replacement materials, which can prevent the plastic deformation of materials in the process of implantation, to ensure stability in bone tissue [51]. The technical standard ASTM F67 divided pure Ti implant into four grades: G1-G4, with YS range of 170-483 MPa and TS of 240-550 Mpa [51]. The YS of Ti alloy (Ti6Al4V) implant is significantly higher than that of pure Ti, and the YS of Ti alloy prepared by different processes is in the range of 360-3267 MPa [52]. The YS and TS of TaNb40 alloy detected in this study were 420 ± 30 MPa and 548 ± 50 MPa respectively,

compared with the pure Ti and Ti alloy recorded in the literature, these two aspects of TaNb40 implant are within the range of mechanical performance indicators, and have good mechanical properties. The Elongation of the TaNb40 alloy is 40%, which is higher than pure Ti and Ti alloy implant based on the relevant literature [51], indicating that the TaNb40 implant has the characteristic of not easy brittle fracture. Besides, compared with Ti material, the Vickers hardness value (425HV) of TaNb40 was higher than that of pure Ti and Ti alloy implant [51]. Hardness refers to the resistance of the material to permanent distortion. It is not too much to say Hardness is an important indicator of wear resistance. Besides, the elastic modulus is also an important property, if it is far greater than that of bone tissue, the difference may produce greater stress at the bone-implant interface in the process of load transmission, resulting in bone loss and implant loosening failure. In our previous studies, through a series of operations such as the design of computer-aided software, the preparation of SLS raw material powder, and the control of processing conditions, the TaNb40 implant was successfully prepared. In this study, the YS and Hardness were preliminarily determined. However, as a medical biomaterial implant, it is still necessary to further detect compressive stress, shear force, elastic modulus, and fatigue strength in the future because the stress in the jaw is very complex, which could provide the basis for adjusting the parameters of 3D printing properly so that all the mechanical properties of the implant can enough to match the bone tissue in vivo.

Good biocompatibility is the prerequisite and foundation of Ta application in the biomedical field. At present, the evaluation of biocompatibility of biomaterials mainly refers to International Organization for Standardization (ISO) 10993 and national standard GB / T16886, including the utilization of different experimental methods in vitro and in vivo. Researchers can choose some of methods to achieve their own research objectives. It can be concluded whether the material conforms to the biological safety and functionality through a series of evaluations, in other words, the material has no toxic effect on the human body and does not cause host heterologous recognition reaction. Besides, the biomaterials should be able to perform the corresponding functions in the specific parts, not be rejected and destroyed, maintain their original physicochemical, mechanical, and biological properties, and have a long-term good combination with the host. Therefore, the other focus of this study is the cytotoxicity of metal materials in vitro. The cytotoxicity test is one important index to evaluate the biocompatibility, which is the most basic experimental method in biological performance evaluation of material. In this study, we observed the effects of TaNb40 and Ta on the morphology, early adhesion, proliferation, and cell cycle of hOMF in vitro, moreover, widely recognized metal pure Ti with good biocompatibility as positive control and pure Ni as negative control were used. After initial implant stability, it is also very necessary to close the soft tissue wound in the second stage of implant surgery, which can promote the healing of soft tissue and prevent the infection caused by a microorganism and other exogenous substances. The healing of oral mucosa soft tissue had to do with the fibroblast proliferation and collagen deposition [53]. Due to the poor antigenicity of fibroblasts and the nonspecificity of antigens, some studies tried to identify fibroblasts based on immunohistochemical staining, but the rate of success rate is very low[54-56]. Therefore, no immunohistochemical method was used to identify fibroblasts in this study. Ultrastructurally, fibroblasts are identified by their stellate appearance with slender branching pseudopods

and have marked rough endoplasmic reticulum(RER) and Golgi complex [57-58]. We observed the hOMF by light microscope, and the results were consistent with the morphology of normal fibroblasts.

To direct observation of the number and morphological changes of the cells in contact with the materials, the direct contact method was used to detect the cytotoxicity. On the 5th day, a small number of apoptotic fragments were observed around the TaNb40、Ta、Ti group, which was the normal apoptosis during the growth of cells. In the Ti group, there was no cell attachment in the area about 0.1 mm around the metal sheet, because the weight of Ti (0.2756g) was less than that of Ta (0.6964g) and TaNb40 (0.7007g) when inoculated with the same volume of culture medium with the same number of cells, Ti would not adhere firmly to the plate due to buoyancy, which affected the surrounding cells to a certain extent. According to the cytotoxicity scoring in vitro, TaNb40, Ta, and Ti were recorded as 0, which did not affect cell growth and had no toxicity to cells. In the Ni group, about 80% of cells were suspended dead cells on the 5th day, the cytotoxicity score was 4, which was considered as a serious toxicity material. Due to the different number and morphology of cells in different distances from the same material, it can be inferred that the cell is affected by some metal elements released from the material, which makes the metal ions distribute unevenly in the culture medium, thus affecting the growth of surrounding cells. Toxicity test is to detect the effects of small molecular substances on cells when materials are degraded or decomposed, the adverse reactions in local tissues are related to the metal ions released by material [59]. Therefore, the cytocompatibility in vitro can also be analyzed by the indirect contact, that is, the extracting liquid method. By ISO 10993-5:2009, the effects of TaNb40, Ta, Ti, and Ni extracting liquid on cell proliferation were tested. CCK-8 can react with enzymes in mitochondria of living cells and display orange-yellow in solution, therefore, the more living cells, the greater the degree of reaction with reagent, the deeper the orange color. The higher the OD value indicating that the cytotoxicity of the material is smaller. The OD value measured by Microplate Reader can reflect the cell activity and cell proliferation. The constant fluctuation of OD values of TaNb40, Ta, and Ti at three-time points may be the unintentional damage to cells caused by the gun head and the error of the testing instrument. The statistical difference between each of the three group and the blank control group indicates that either these three materials do have a slight impact on cells, or the initial number of cells in the blank control group is more than that in the TaNb40, Ta and Ti group due to the counting error, so go a step further analysis the cell cycle distribution. Although there was the statistical difference, the cytotoxicity analysis showed that TaNb40, Ta, and Ti did not produce cytotoxicity, and the grade was 1, which met the requirements of medical biomaterials. However, the OD value of the Ni group was lower than 0.5 at the outset, and the cell proliferation was inhibited over time, which was consistent with the results of direct contact morphological analysis. The cytotoxicity of the Ni group was grade 3, which did not conform to the standard of medical biomaterials.

The surface properties of the material, such as surface energy, hydrophobicity/hydrophilicity, net charge, and roughness, affect the adsorption of cells and macromolecules on the surface after implantation [60]. To observe the effect of the surface properties on the early adhesion of hOMF, an AO reagent was used to stain cells and observe the early cell adhesion at the 4th, 6th, and 12th hour. AO is a fluorescent dye used

to observe the number of adhesion cells on the surface of opaque material, the reagents emit different colors of fluorescence by binding with nuclear DNA and RNA, so the adhesion ability of cells can be evaluated. The cell adhesion rate of TaNb40, Ta, and Ti group increased with time, and the maximum was found at the 12th hour, the TaNb40 and Ta increased significantly at three-time points ($P < 0.01$), indicating that they did not affect the cell adhesion. Compared with the other three groups, the initial adhesion rate of the Ni group was very low, and as time goes on, not only no cells attached, but also the cells adhering on the surface of the material also showed lysis apoptosis, and the adhesion rate was lower. At the 4th hour, the cell adhesion rate of the Ti group was higher than that of TaNb40 and Ta group ($P < 0.05$), at the 6th and 12th hour, the TaNb40 and Ta were higher than that of the Ti group, and the difference was statistically significant ($P < 0.01$), which make clear that the initial adhesion of cells of the TaNb40 and Ta is better than that of Ti, and can quickly stick to the surface in the early stage, this result may be related to the roughness surface prepared by SLS technology. Studies have shown that the surface topography (flat, rough, nanometer) and crystal size of biomaterials affect the interaction between cell and material interface, and then have an effect on their biological characteristics [61]. The low level of cell differentiation in the flat morphology might be due to its more inert surface, resulting in less cellular reaction [62]. The roughness of the nanoparticle size can intervene in the behavior of the cells. Some scholars [63-64] prepared bulk ultrafine-grained pure Ta by Equal Channel Angular Pressure (ECAP), after treatment, the number of grain boundaries on the surface increased, providing more cell adhesion sites, showing better cell activity and biocompatibility. The nano pits can change the surface roughness, wettability, and the adsorption capacity of fibronectin, it could also be recognized by fibroblasts, especially when the size of nano pits is 50 nm and 60 nm respectively, which can significantly enhance the attachment and proliferation of fibroblasts [65]. The TaNb40 surface showed a certain roughness whose pit size could not be determined due to without measurement of the surface microstructure. It can be seen that the early adhesion rate of cells on the rough surface of TaNb40 prepared by SLS is higher than that on the Ti surface from our experimental results, but the error in the operation is also not ruled out, which is related to the inherent chemical properties of Ta surface. Some scholars have studied the effect of inherent chemical properties of Ti and Ta on Bone Marrow Mesenchymal Stem Cells (BMSCs), the results showed that the expression of integrin α5 and β1 on Ta surface was higher. Integrin plays an important role in the formation of focal adhesion complex, mediates intracellular signal transduction, and regulates the process of cell differentiation [66]. Other studies have shown that [44-46] Ta has better osteogenic differentiation than Ti in prosthesis and implant coating. The surface characteristics of materials, such as surface structure and physicochemical properties, can significantly affect the behavior of cells and subsequently bone induction and osseointegration. At the 12th hour, the average number of adherent cells on the Ta and TaNb40 group was more than 100%, indicating that not only the number of adherent cells on the surface of the material increased significantly but also some cells were in the early stage of proliferation at this time point. In a word, the TaNb40 implant or disk-shaped material made by SLS has no surface treatment, which does has better cell adhesion, even better than Ti. Therefore, it can be inferred that it may not require further surface treatment, and the relatively rough surface is conducive to cell adhesion and growth.

To determine whether the cell cycle was blocked by different materials and which cell cycle stage is inhibited by Ni, the cells were stained with Propidium Iodide (PI), so the DNA content was detected by flow cytometry. Various cell cycle stages have different DNA ploidy numbers, according to the distribution of cells in each phase of the cell cycle, we can judge whether the materials have no, promote or inhibit proliferation effect on cells. The cells were treated with the extracting liquid after 48 hours. Compared with the blank control group, the percentage of G1 / S phase cells in the Ta group tended to increase, the G2 phase decreased, indicating that DNA synthesis accelerated, thus promoting DNA replication and cell proliferation. In the TaNb40 group, the results indicated that the cells were in normal growth and proliferation stage. In the Ti group, the G1 phase decreased and S / G2 phase increased, the cells were in G1 to S phase transformation stage combined with cell proliferation results, which promoted cell proliferation. The cell proliferation results between the TaNb40, Ta, Ti, and blank control at three- time points were statistically different ($P < 0.01$), but there was no cell cycle arrest. The possible reason is that the initial number of cells in the blank control group was more than that in these three groups due to the error of cell count, thereby displaying the statistical difference of OD value in each group. Compared with 3.11% of the blank control group, the percentage of S-phase cells increased significantly in the Ni group, and 3.91% of cells in the sub-G1 phase were apoptotic. Therefore, Ni induced cell cycle arrest in the S phase and promoted cell apoptosis in this study. The ion content of Ni extracting liquid was 264mg/kg. Qiao et al. [67] found that 10 um Ni could cause DNA damage in vitro. Besides, it also was found that [68] Ni nanoparticles (NiNPs, size: 28nm) decreased the survival rate of human liver (HepG2) cells in a dose-dependent manner in the concentration range of 25-100μg / ml. DNA damaged cells accumulate at Gap1 (G1), DNA synthesis (s), or Gap2 / Mitosis (G2/M). Studies have shown that [68-69] Nickel chloride ($NiCl_2$) induces G2 / M arrest of the liver. A large number of metal ions accumulated in the body can induce a series of pro-inflammatory reactions. A kind of metal ion can activate a variety of intracellular signaling pathways to mediate the release of cytokines, promote the formation of the local inflammatory response and initiate cell apoptosis mediated by mitochondria. If this immune- inflammatory reaction persists, osteolysis will eventually occur, resulting in implant loosening and fracture. The long-term wear of artificial joints and the particles produced by dissociation in the humoral environment will lead to the above phenomenon. In this study, the ion contents in the different extracting liquids were further measured. Except for Ni ions, almost no metal ions were detected in other groups. The amount of metal ions precipitated in TaNb40 and Ta group was less than 0.1mg/kg, and the Ti was less than 0.2mg/kg. The number of the released metal elements is closely related to the properties of surface passivation oxide film and corrosion resistance. Many references [70-72] have proved that the passivation oxide film on the surface of Ta is very stable, and no corrosion sign has been found in physiological solution in vitro. Two kinds of passive oxide films, Ta_2O_5 and Nb_2O_5, exist on the surface of TaNb40, which has excellent corrosion resistance [72]. The corrosion resistance of Ni is very poor, the stability of surface film NiO is low, and a large amount of Ni ion [73-74] can be released in a short time. Therefore, Ta and TaNb40 have excellent corrosion resistance and biocompatibility. At least there is almost no metal ion release in vitro. The poor biocompatibility of Ni is related to the instability of surface passive film and the release of Ni.

Conclusions

TaNb40 implant was prepared by SLS technology of 3D printing in our previous studies, its surface is bright gray, showing a certain degree of roughness. (1) The TS, YS, Elongation, and Vickers hardness was 548 ± 50MPa, 420 ± 30MPa, 40%, and 425HV respectively, which indicate that the TaNb40 implant has good mechanical properties, wear-resistance, and not easy to brittle fracture. (2) TaNb40 and Ta were tested in vitro by direct contact, AO fluorescence staining, CCK-8, and flow cytometry, it was found that the two materials did not inhibit cell proliferation and cell cycle arrest, the cytotoxicity grade in vitro was 1. There was almost no metal ion release in the culture medium, and both of them have good early cell adhesion ability. All above these, it meets the requirements of medical biomaterials. (3) In general, the mechanical properties and cell compatibility in vitro of TaNb40 are excellent, which is expected to replace the Ti implant prepared by the traditional casting method. It is of guiding significance for the research and development of implant materials with independent intellectual property rights.

However, the stress on the implant in the jaw is very complex, which is still necessary to detect the compressive stress, shear force, elastic modulus, fatigue strength in the future, to provide the basis for timely adjusting the parameters of 3D printing, and make the mechanical properties of the implant match the bone tissue in vivo. In terms of the biological performance evaluation, the osteogenic of cells on the surface of materials and the osseointegration in animals also need to be further studies in the future.

Preparation of experimental materials

The CT Scanning (FS271M, Hunan Huashu High Tech Co., Ltd) appearance parameters of the TaNb40 sample (Changsha Nanfang Tantalum Niobium CO, LTD, China) was set according to commonly used Ti alloy (Basic implant system, USA) implant in the clinic. The chemical composition of TaNb40 suitable for SLS in this experiment is Ta: Nb = 5.8 ~ 6.2 : 3.8 ~ 4.2. The composition and proportion of residual elements are shown in Table 6, and the totality weight ratio is less than 1.5%, the particle size of Ta and Nb powder is 10μm-60μm, and the SLS laser power is 250W. To facilitate the co-culture of the cells with materials in the same culture dish, the Ta-Nb alloy sheet, or TaNb40 for short (9 mm in diameter and 1 mm in thickness) was prepared by SLS. At the same time, Ta sheet with the same size was prepared by traditional casting method as another experimental group, and Ti and Ni sheet (Yudingda Metal, China) was used as positive and negative control materials respectively. The materials were sterilized by high temperature and high pressure.

Characterization of materials

In this project, the test of mechanical properties of TaNb40 includes TS and Vickers hardness. Five samples were used for each index. According to the national standard GB / T1040, the tensile properties of TaNb40 alloy were tested by a Tensile testing machine (Shanghai Hesheng Instrument Technology Co., Ltd) at room temperature. Besides, the unit stress on the indentation area was measured by Vickers hardness tester (Shanghai Jujing Precision Instrument Manufacturing Co., Ltd) according to the GB / T 4340.1-2009.

Primary culture of human Oral Mucosa Fibroblasts

This study was approved by the ethics committee of Xiangya School of Stomatology, Central South University, with the approval number of 20190015. The human Oral Mucosa Fibroblasts (hOMF) strain (set up by the author's team) were established as experimental cells. The third generation of hOMF was taken out from liquid nitrogen and the cells after resuscitation were cultured in an incubator (ThermoFisher) containing 5% CO2 and 37 ℃ / 95% humidity until it grows to 80% - 90%, then going down to the future generation.

The cell growth observed by the direct contact method

The experiment was divided into five groups: TaNb40, Ta, Ti, Ni, and blank control group (only cells without material). It was proper in the density of 3×10^4 cell/ml, each group of materials setting up four parallel groups was placed in a 24-pore plate (Excell Bio, China) to co-culture with the cells. On the 1st, 3rd, and 5th day, the cell growth around the material was observed by an inverted microscope(Leica). According to the national standard GB / T 16886.5, the cytotoxicity in vitro score was recorded taking 100% of the number of cells in the blank control group as the benchmark. Such as the following: 0. No cytotoxicity, no effect on cell growth; 1. Slight cytotoxicity, the number of round cells ≤ 20%; 2. 20% < the number of round cells ≤ 50%, with slight cell growth inhibition; 3. 50% < the number of rounds or dissolved cells ≤ 70%; 4. Severe cytotoxicity, resulting in serious cell damage.

The early cell adhesion observed by AO fluorescence staining

The experiment was divided into four groups: TaNb40, Ta, Ti, and Ni group. Acridine Orange (AO) fluorescence staining (BestBio, China) was used to observe the early cell adhesion on the surface of the material (within 12 hours). Collecting the sample cells, counting, the cell density was about 2×10^5/ml, and the 50ul cell suspension was added to the different material surfaces. After 30 minutes of cell sedimentation, adding 0.5ml culture medium again. The 50 ul of dye solution was added to the surface after the 1st day and 4th day respectively and incubated for 10-15 minutes in dark at 4 ℃. The maximum excitation wavelength was 488 nm.

Using Image J software, five visual fields were randomly selected for each sample under the microscope, finally set up the database, perform statistical analysis.

Prepare the extracting liquid

According to the national standard ISO 10993-5:2009, the material extracting liquid was prepared according to the ratio of the extraction medium and the surface area (or weight) of the biomaterial. In this experiment, the sample diameter is 9mm and the thickness is 1mm, the extraction ratio is $3 / cm^2 \cdot ml^{-1}$ based on Table 7. It is calculated that 0.53ml culture medium should be added to the 24-well plate containing materials, and placed in the refrigerator(ThermoFisher) at 4 ℃ as the extracting liquid.

The cell proliferation determined by CCK-8

The experiment was divided into five groups: the extracting liquid of TaNb40, Ta, Ti, Ni, and the blank control group. The cell density was about 3×10^4 cells/ml. Each group of materials was put into a 96-well plate (Excell Bio, China), dropping 100ul cell suspension, after 24 hours, discarding the old culture medium, and adding 100μl per experiment group. After the 1st, 3rd, and 5th day, add 10ul CCK-8 reagent (BestBio, China).

The OD value of each pore was measured by enzyme-labeled instrument (Thermo Scientific Multiskan FC) at 450 nm. The OD value of the blank control group was taken as the standard, and the relative growth rate (RGR) was calculated by the ratio of OD mean value of experiment groups to that of the blank control group. RGR (%) = ODsample / ODblank × 100%. The cytotoxicity evaluation grading is shown in Table 8.

Cell cycle determined by flow cytometry

The experimental groups were the extracting liquid of TaNb40 and Ta, the control groups were the extracting liquid of Ti, Ni, and the blank control group(the complete medium). The number of cells in each group was about (5-10) × 10^6. The 3.5 ml of cold ethanol (Excell Bio, China) was slowly dropped into each tube(Excell Bio, China) with cells, and the final concentration of ethanol was about 75%. The samples were fixed overnight at 4 ℃ and stored at - 20 ℃. Within one week, the 400 UL PI staining solution(BestBio, China) was added to resuspend the cells. Results were detected by flow cytometry(BD, USA), the excitation wavelength was 488 nm, and Cell DNA content, light scattering were analyzed by ModFit software.

Determination of metal ions in the extracting liquid

The contents of metal ions in each group were determined by Inductively Coupled Plasma mass spectrometry (ICP-MS) (NCS Testing Technology Co., Ltd). The text process was shown in Fig. 11.

Abbreviations

SS: Stainless Steel; Ti: Titanium; TiZr: Titanium-Zirconium; Al: Aluminum; V: Vanadium; Ta: Tantalum; PTTM: Porous Tantalum Trabecular Metal; Nb: Niobium; SLA: Stereolithography; FDM: Fused Deposition Modeling; SLS: Selective Laser Sintering; 3DP: Three-dimensional printing; CAD: Computer-Aided Design; TS: Tensile Strength; hOMF: human Oral Mucosa Fibroblasts; AO: Acridine Orange; RGR: Relative Growth Rate; ICP-MS: Inductively Coupled Plasma Mass Spectrometry; YS: Yield Strength; ISO: International Organization for Standardization; RER: Rough Endoplasmic Reticulum; ECAP: Equal Channel Angular Pressure; BMSCs: Bone Marrow Mesenchymal Stem Cells; PI: Propidium Iodide.

Declarations

Acknowledgments

Thanks to Xiangya Medical Science Research Center of Central South University for the technical support of this study.

Funding

This research was funded by “2017 Key Research and Development Program of Hunan Province in China(Grant. No.2017GK2265)”, “2018 Key Research and Development Program of Hunan Province in China(Grant. No.2018SK2104)” and “Department of health project of Hunan Province in China, grant number (Grant. No.B2015-142).

Availability of data and materials

The data sets used and/or analyzed during the current study are available from the corresponding author on reasonable request.

Author Contributions

methodology, writing—original draft preparation, writing—review and editing, data curation, Huiling Li;

Conceptualization, validation, Junhui Huang and Zhigang Yao;

resources, visualization, Jian Zhang;

All authors have read and agreed to the published version of the manuscript.

Ethics approval and consent to participate

This study was approved by the ethics committee of Xiangya School of Stomatology, Central South University, with the number 20190015.

Consent for publication

Not applicable.

Competing interests

The author(s) declared no potential conflicts of interest concerning the research, authorship, and/or publication of this article.

Patents

Part of the work in this study has applied patent for invention: (1) A 3D-printing method of Tantalum-Niobium alloy dental implant, patent number: 201910208621.1; (2) A Tantalum-Niobium alloy dental

implant and preparation, patent number: 201910208701.7; (3) A Tantalum-Niobium alloy dental implant material and a Tantalum-Niobium alloy dental implant, patent number: 201910209344.6.

References

1. Zou X, Li H, Bünger M, et al. Bone ingrowth characteristics of porous tantalum and carbon fiber interbody devices: an experimental study in pigs[J]. The Spine Journal. 2004; 4(1): 99-105.
2. Milleret V, Lienemann PS, Gasser A, et al. Rational design and in vitro characterization of novel dental implant and abutment surfaces for balancing clinical and biological needs[J]. Clin Implant Dent Relat Res. 2019; Suppl 1:15-24.
3. Al-Rabab'ah M, Hamadneh W, Alsalem I, et al. Use of High Performance Polymers as Dental Implant Abutments and Frameworks: A Case Series Report[J]. J Prosthodont. 2019; 28(4):365-372.
4. Sandhaus S. Technic and instrumentation of the implant C.B.S. (Cristalline Bone Screw)[J]. Inf Odontostomatol. 1968; 4(3):19-24.
5. Andreiotelli M, Kohal RJ. Fracture strength of zirconia implants after artificial aging[J]. Clin Implant Dent Relat Res. 2009; 11(2):158-166.
6. Lang NP, Pjetursson BE, Tan K, et al. A systematic review of the survival and complication rates of fixed partial dentures (FPDs) after an observation period of at least 5 years. II. Combined tooth–implant-supported FPDs[J]. Clin Oral Implants Res. 2004; 15(6):643-653.
7. Moraschini V, Poubel LA, Ferreira VF, et al. Evaluation of survival and success rates of dental implants reported in longitudinal studies with a follow-up period of at least 10 years: a systematic review[J]. Int J Oral Maxillofac Surg. 2015; 44:377–388.
8. Nelson C. Factors Affecting the Success of Dental Implants. In:Turkyilmaz I, ed. Implant Dentistry – A Rapidly Evolving Practice[J]. 1st ed. London: IntechOpen. 2011; 319–364.
9. Hanawa T, Tsutsumi Y. Calcium phosphate formation on titanium and zirconium and its application to medical devices[J]. Bioceram Dev Apl. 2010; 1:1–4.
10. Gottlow J, Dard M, Kjellson F, et al. Evaluation of a new titanium-zirconium dental implant: a biomechanical and histological comparative study in the mini pig[J]. Clin Implant Dent Relat Res. 2012; 14(4):538-545.
11. van Velzen FJ, Ofec R, Schulten EA, et al. 10-year survival rate and the incidence of peri-implant disease of 374 titanium dental implants with a SLA surface: a prospective cohort study in 177 fully and partially edentulous patients[J]. Clin Oral Implants Res. 2015; 26(10):1121-1128.
12. Yu Y, Jin G, Xue Y, et al. Multifunctions of dual Zn/Mg ion co-implanted titanium on osteogenesis, angiogenesis and bacteria inhibition for dental implants[J]. Acta Biomater. 2017; 49:590-603.
13. Siddiqui DA, Guida L, Sridhar S, et al. Evaluation of oral microbial corrosion on the surface degradation of dental implant materials[J]. J Periodontol. 2019; 90(1):72-81.
14. Iegami CM, Uehara PN, Sesma N, et al. Survival rate of titanium-zirconium narrow diameter dental implants versus commercially pure titanium narrow diameter dental implants: a systematic review[J].

Clin Implant Dent Relat Res. 2017; 19(6):1015–1022.

15. Medvedev AE, Molotnikov A, Lapovok R, et al. Microstructure and mechanical properties of Ti–15Zr alloy used as dental implant material[J]. J Mech Behav Biomed Mater, 2016, 62:384–398.
16. Akimoto T, Ueno T, Tsutsumi Y, et al. Evaluation of corrosion resistance of implant-use Ti-Zr binary alloys with a range of compositions[J]. J Biomed Mater Res Part B Appl Biomater. 2018; 106:73–79.
17. Zhao B, van der Mei HC, Rustema-Abbing M, et al. Osteoblast integration of dental implant materials after challenge by sub-gingival pathogens: a co-culture study in vitro[J]. Int J Oral Sci. 2015; 7(4):250–258.
18. Gahlert M, Röhling S, Wieland M, et al. Osseointegration of zirconia and titanium dental implants: a histological and histomorphometrical study in the maxilla of pigs[J]. Clin Oral Implants Res. 2009; 20:1247–1253.
19. Depprich R, Zipprich H, Ommerborn M, et al. Osseointegration of zirconia implants: an SEM observation of the bone-implant interface[J]. Head Face Med. 2008; 4:25.
20. Hallmann L, Mehl A, Ulmer P, et al. The influence of grain size on low-temperature degradation of dental zirconia[J]. J Biomed Mater Res Part B Appl Biomater. 2012; 100(2):447–456.
21. Osman R, Swain M. A critical review of dental implant materials with an emphasis on titanium versus zirconia[J]. Materials (Basel). 2015; 8(3):932–958.
22. Han CX. Study on Refractory Metal Materials[J]. SCIENCE & TECHNOLOGY INFORMATION. 2013; 15: 89.
23. Yu CY, YuYJ. Alien Metal titanium zirconium tantalum[J]. Rare Metals Letters. 2004; 23:31-34.
24. Hu ZW, Li ZK, Zhang TJ. New development and application of tantalum and tantalum alloy[J]. Rare Metals and Cemented Carbides. 2003; 31(3):34-36.
25. Brett R L, Scott S, Robert A P, et al. Experimental and clinical performance of porous tantalum in orthopedic surgery[J]. Biomaterials. 2006; 27(27): 4671–4681.
26. Lee GW, Park KS, Kim DY, et al. Results of Total Hip Arthroplasty after Core Decompression with Tantalum Rod for Osteonecrosis of the Femoral Head[J]. Clinical in Orthopedic Surgery. 2016; 8(1): 38-44.
27. Sagherian BH, Claridge RJ. Salvage of Failed Total Ankle Replacement Using Tantalum Trabecular Metal: Case Series[J]. Foot & Ankle society. 2015; 36(3): 318-324.
28. King V, Swart A, Winder MJ, et al. Tantalum trabecular metal implants in anterior cervical corpectomy and fusion: 2-year prospective analysis[J]. J Clin Neurosci. 2016; 32: 91-94.
29. Konan S, Duncan CP, Masri BA, et al. Porous tantalum uncemented acetabular components in revision total hip arthroplasty[J]. Bone Joint J. 2016; 98-B(6):767-771.
30. Wang H, Li J, Yang H, et al. Fabrication, characterization and in vitro biocompatibility evaluation of porous Ta–Nb alloy for bone tissue engineering[J]. Mater Sci Eng C Mater Biol Appl. 2014; 40:71–75.
31. Liu J, Chang L, Liu H, et al. Microstructure, mechanical behavior and biocompatibility of powder metallurgy Nb-Ti-Ta alloys as biomedical material[J]. Mater Sci Eng C Mater Biol Appl. 2017; 71:

512–519.

32. Liaw CY, Guvendiren M. Current and emerging applications of 3D printing in medicine[J]. 2017; 9(2):024102.
33. Giovinco NA, Dunn SP, Dowling L, et al. A novel combination of printed 3-dimensional anatomic templates and computer-assisted surgical simulation for virtual preoperative planning in charcort foot reconstruction[J]. J Foot Ankle Surg. 2012; 51:387-393.
34. He CL TangCH Tian HY Chen XS. Research progress of biomedical polymer materials prepared by 3D printing technology[J]. Acta Polym Sin. 2013; 6:31-34.
35. Das S. Physical aspects of process control in selective laser sintering of metals[J]. Adv Eng Mater. 2003; 5(10):701– 711.
36. Fina F, Goyanes A, Gaisford S, et al. Selective laser sintering (SLS) 3D printing of medicines[J]. International Journal of Pharmaceutics. 2017; 529(1-2):285–293.
37. Goyanes A, Buanz ABM, Hatton GB, et al. 3D printing of modified-release aminosalicylate (4-ASA and 5-ASA) tablets[J]. Eur. J. Pharm. Biopharm. 2015; 89:157–162.
38. Goyanes A, Robles Martinez P, Buanz A, et al. Effect of geometry on drug release from 3D printed tablets[J]. Int. J. Pharm. 2015; 494(2): 657–663.
39. Okwuosa TC, Pereira BC, Arafat B, et al. Fabricating a shell-core delayed release tablet using dual FDM 3D printing for patient-centered therapy[J]. Pharm. Res. 2017; 34(2):427–437.
40. Brito NM, Soares RS, Monteiro EL, et al. Additive Manufacturing for Surgical Planning of Mandibular Fracture[J]. Acta Stomatol Croat. 2016; 50(4):348-353.
41. Mafeld S, Nesbitt C, McCaslin J, et al. Three-dimensional (3D) printed endovascular simulation models: a feasibility study[J]. Ann Transl Med. 2017; 5(3):42.
42. Ren X, Yang L, Duan XJ. Three-dimensional printing in the surgical treatment of osteoid osteoma of the calcaneus: A case report. J Int Med Res. 2017; 45(1):372-380.
43. Tetsworth K, Block S, Glatt V. Putting 3D modeling and 3D printing into practice: virtual surgery and preoperative planning to reconstruct complex post-traumatic skeletal deformities and defects[J]. SICOT J. 2017; 3:16-19.
44. Tang Z, Xie Y, Yang F, et al. Porous Tantalum Coatings Prepared by Vacuum Plasma Spraying Enhance BMSCs Osteogenic Differentiation and Bone Regeneration In Vitro and In Vivo[J]. PLoS ONE. 2013; 8(6): e66263.
45. Stiehler M, Lind M, Mygind T, et al. Morphology, proliferation, and osteogenic differentiation of mesenchymal stem cells cultured on titanium, tantalum, and chromium surfaces[J]. J Biomed Mater Res. 2008; 86(2): 448–458.
46. Hofstetter W, Sehr H, de Wild M, et al. Modulation of human osteoblasts by metal surface chemistry[J]. J Biomed Mater Res Part A. 2013; 101(8):2355–2364.
47. Lee JW, Wen HB, Gubbi P, et al. New bone formation and trabecular bone microarchitecture of highly porous tantalum compared to titanium implant threads:A pilot canine study[J]. Clin Oral Impl Res.

2018; 29(2):164–174.

48. Datta S, Mahfouf M, Zhang Q, et al. Imprecise knowledge based design and development of titanium alloys for prosthetic applications. J Mech Behav Biomed Mater. 2016; 53:350–365.
49. Ramírez G, Rodil SE, Arzate H, et al. Niobium based coatings for dental implants. Appl Surf Sci. 2011; 257(7):2555–2559.
50. Mohammed MT, Khan ZA, Geetha M, et al. Microstructure, mechanical properties and electrochemical behavior of a novel biomedical titanium alloy subjected to thermomechanical processing including aging. J Alloys Compd. Elsevier B.V. 2015; 634:272–280.
51. Elias CN, Fernandes DJ, Resende CRS, et al. Mechanical properties, surface morphology and stability of a modified commercially pure high strength titanium alloy for dental implants. Dent Mater. 2015; 31(2):e1–13.
52. Cordeiro JM, Barão VAR. Is there scientific evidence favoring the substitution of commercially pure titanium with titanium alloys for the manufacture of dental implants? Mater Sci Eng C Mater Biol Appl. 2017; 71:1201-1215.
53. Woodley DT. Distinct Fibroblasts in the Papillary and Reticular Dermis: Implications for Wound Healing[J]. Dermatol Clin. 2017; 35(1): 95–100.
54. Wilkinson LS, Pitsillides AA, Worrall JG, et al. Light microscopic characterisation of the fibroblast-like synovial intimal cell (Synoviocyte)[J]. Arthrit. Rheum. 1992; 35(10): 1179–1184.
55. Bachmann S, Le Hir M, Eckardt KU. Co-localization of erythropoietin mRNA and ecto-50-nucleotidase immunoreactivity in peritubular cells of rat renal cortex indicates that fibroblasts produce erythropoietin[J]. J. Histochem. Cytochem. 1993; 41(3): 335–341.
56. Strutz F, Okada H, Lo CW, et al. Identification and characterisation of a fibroblast marker—FSP1[J]. J. Cell Biol. 1995; 130(2): 393–405.
57. Takahashi-Iwanaga H. The three-dimensional cytoarchitecture of the interstitial tissue in the rat kidney[J]. Cell Tissue Res. 1994; 264(2): 269–281.
58. Sappino AP, Schürch W, Gabbiani G. DiVerentiation repertoire of fibroblastic cells: Expression of cytoskeletal proteins as a marker of phenotypic modulations[J]. Lab Invest. 1990; 63(2): 144–161.
59. Żebrowski R, Walczak M, Korga A, et al. Effect of Shot Peening on the Mechanical Properties and Cytotoxicity Behaviour of Titanium Implants Produced by 3D Printing Technology[J]. J Healthc Eng. 2019; 2019:8169538.
60. Talha M, Ma Y, Kumar P, et al. Role of protein adsorption in the biocorrosion of metallic implants - A review[J]. Colloids Surf B Biointerfaces. 2019; 176:494-506.
61. Li YL, Zhang S, Guo LJ, et al. Collagen coated tantalum substrate for cell proliferation[J]. Colloids Surf B. 2012; 95:10-15.
62. Anwar IB, Santoso A, Saputra E, et al. Human Bone Marrow-Derived Mesenchymal Cell Reactions to 316L Stainless Steel: An in Vitro Study on Cell Viability and Interleukin-6 Expression[J]. Adv Pharm Bul. 2017; 7(2): 335-338.

63. Huo WT, Zhao LZ, Yu S, et al. Significantly enhanced osteoblast response to nano-grained pure tantalum[J]. Sci Rep. 2017; 7:40868.
64. Nie FL, Zheng YF, Wang Y, et al. Microstructures, mechanical behavior, cellular response, and hemocompatibility of bulk ultrafine-grained pure tantalum[J]. J Biomed Mater Res B Appl Biomater. 2014; 102(2):221-230.
65. Ni SY, Sun LL, Ercan B, et al. A mechanism for the enhanced attachment and proliferation of fibroblasts on anodized 316L stainless steel with nano-pit arrays[J]. J Biomed Mater Res Part B. 2014; 102(6):1297–1303.
66. Lu MM, Zhuang XH, Tang KW, et al. Intrinsic Surface Effects of Tantalum and Titanium on Integrin α5β1/ERK1 1/2 Pathway-Mediated Osteogenic Differentiation in Rat Bone Mesenchymal Stromal Cells[J]. Cell Physiol Biochem. 2018; 51(2):589-609.
67. Qiao Y, Ma L. Quantification of metal ion induced DNA damage with single cell array based assay[J]. 2013; 139(19): 5713–5718.
68. Ahmad J, Alhadlaq HA, Siddiqui MA, et al. Concentration-dependent induction of reactive oxygen species, cell cycle arrest and apoptosis in human liver cells after nickel nanoparticles exposure[J]. Environ Toxicol. 2015; 30(2):137-148.
69. Guo H, Cui H, Fang J, et al. Nickel chloride (NiCl2) in hepatic toxicity: apoptosis, G2/M cell cycle arrest and inflammatory response[J]. Aging (Albany NY). 2016; 8(11):3009-3027.
70. Levine BR, Sporer S, Poggie RA, et al. Experimental and clinical performance of porous tantalum in orthopedic surgery[J]. Biomaterials. 2006; 27(27):4671–4681.
71. Hee AC, Cao HI, Zhao Y, et al. Cytocompatible tantalum films on Ti6Al4V substrate by filtered cathodic vacuum arc deposition[J]. Bioelectrochemistry. 2018; 122:32-39.
72. Li HZ, Zhao X, Xu J. MRI-compatible Nb–60Ta–2Zr alloy for vascular stents: Electrochemical corrosion behavior in simulated plasma solution[J]. Mater Sci Eng C Mater Biol Appl. 2015; 56: 205–214.
73. Herting G, Wallinder IO, Leygraf C. Metal release rate from AISI 316L stainless steel and pure Fe, Cr and Ni into a synthetic biological medium- a comparison[J]. J. Environ. Monit. 2008; 10(9): 1092–1098.
74. Muñoz AG, Benitez G, Vela ME, et al. Influence of the Adsorption of N Species on the Anodic Dissolution of Ni[J]. Langmuir. 2004; 20(6):2361-2368.

Figures

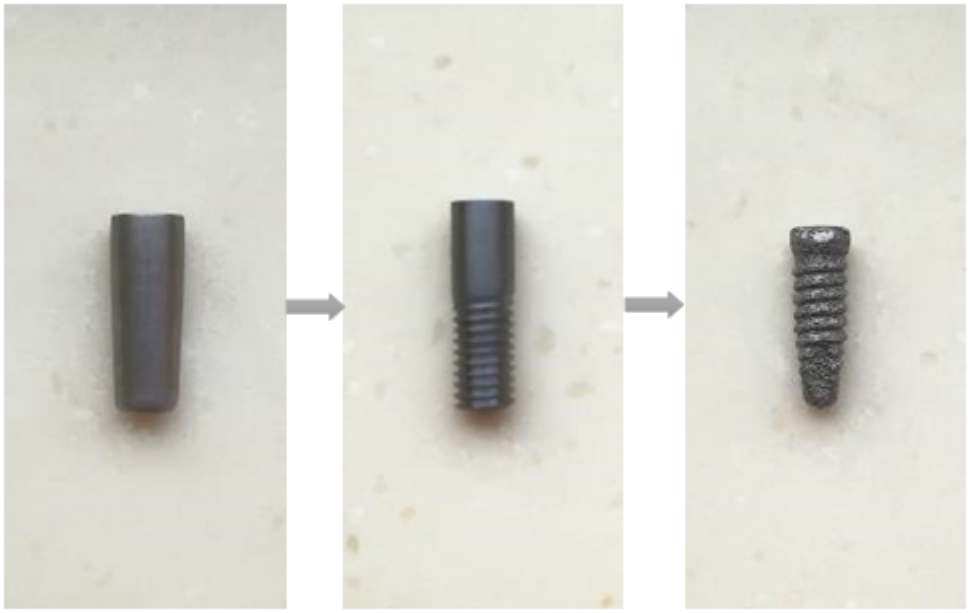

Figure 1

Ta-Nb alloy mplant prepared by SLS

Figure 2

Titanium alloy impiant commonly used in the clinic

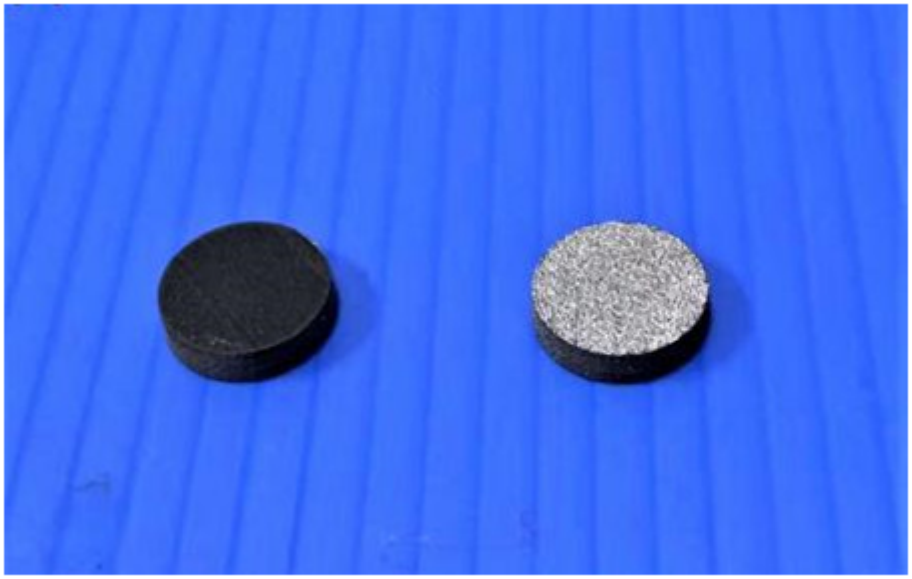

Figure 3

The TaNb40 alloy disc made by SLS

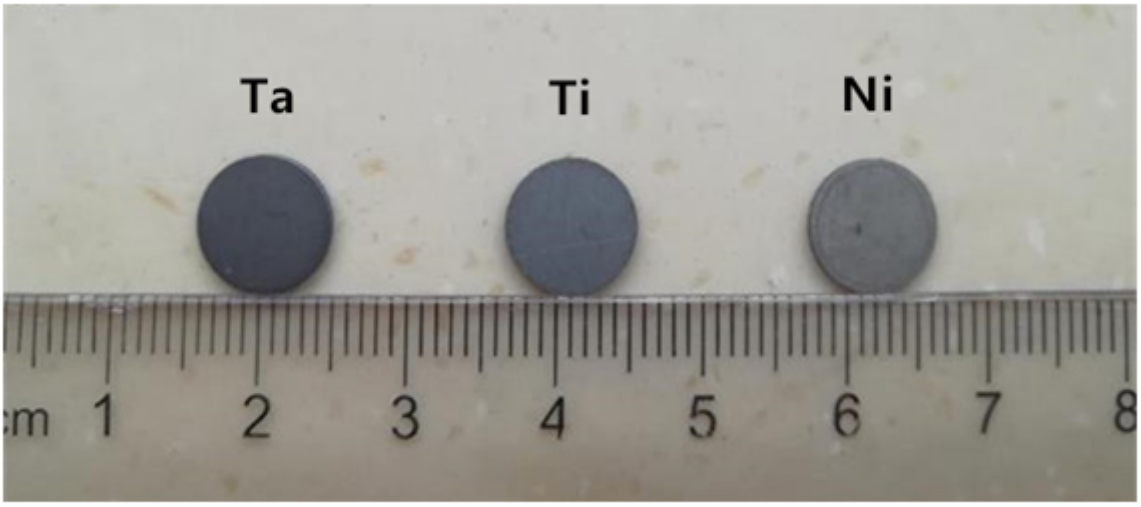

Figure 4

The Ta, Ti, and Ni experimental materials used by radibonal casting method

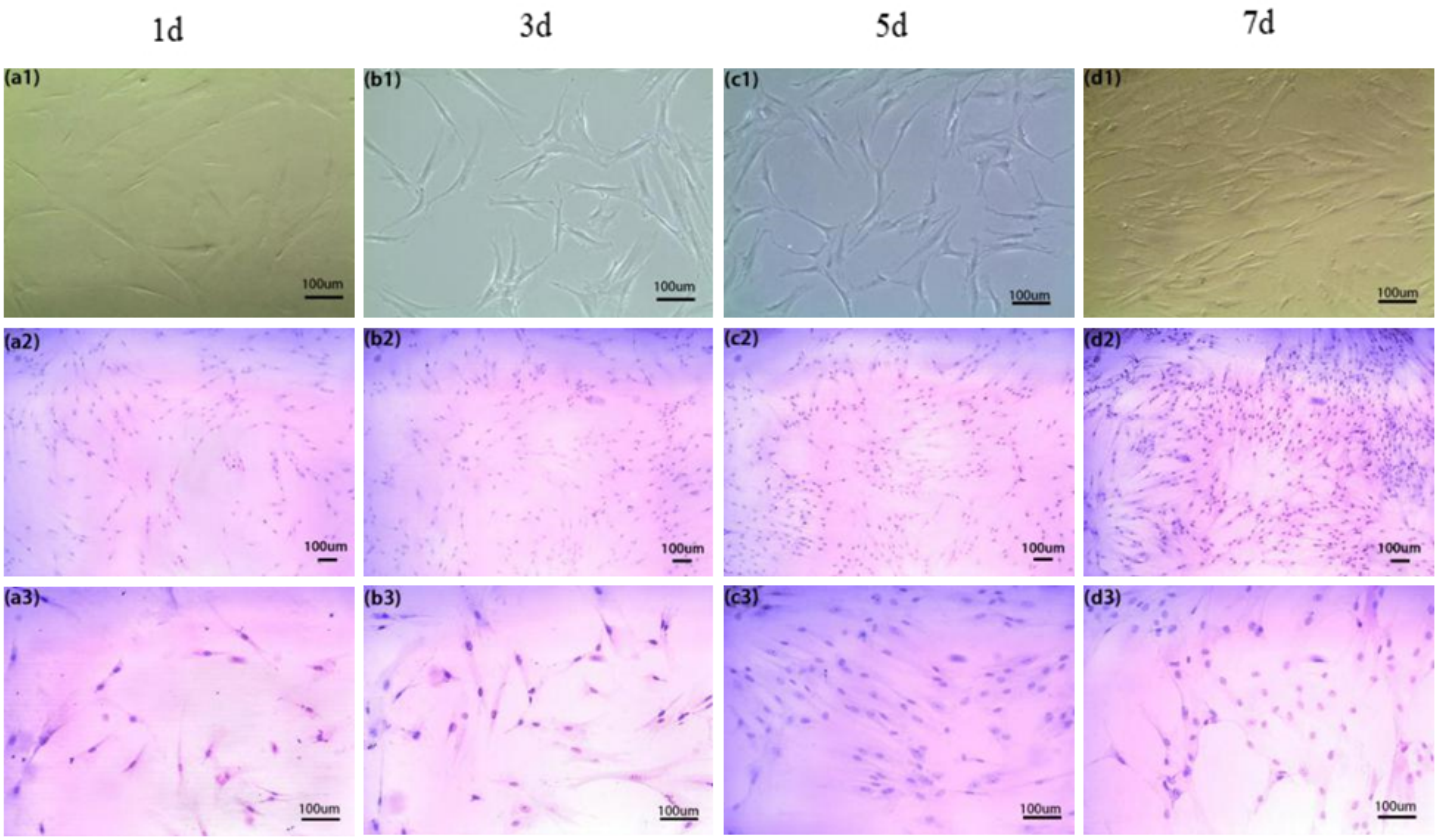

Figure 5

The hOMF of the 5” - 6” generation, (a1)-(d1) (x 100) show the cell morphology under an inverted microscope ; (a2)-(d2) (x40) and (a3)-(d3) (x 100) show the cell morphology under a bght microscope

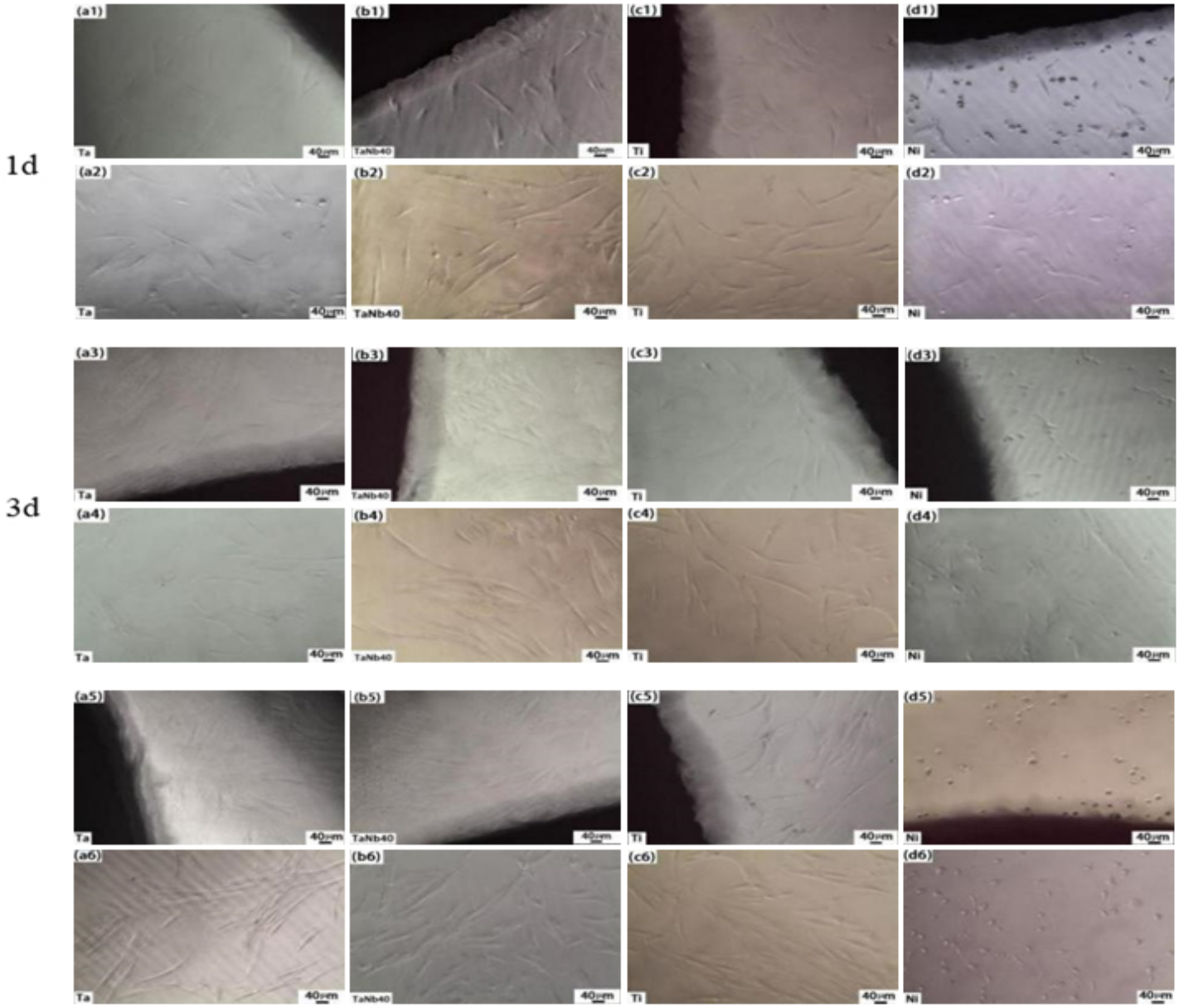

Figure 6

The cells growth around different materials on the 1st, 3rd, and 5th day, (a1)-(d1) (a3)-(d3) (a5)-(d5) show cells around materials; (a2)-(d2) (a4)-(d4) (a6)-(d6) show cells relatively far away fom materials

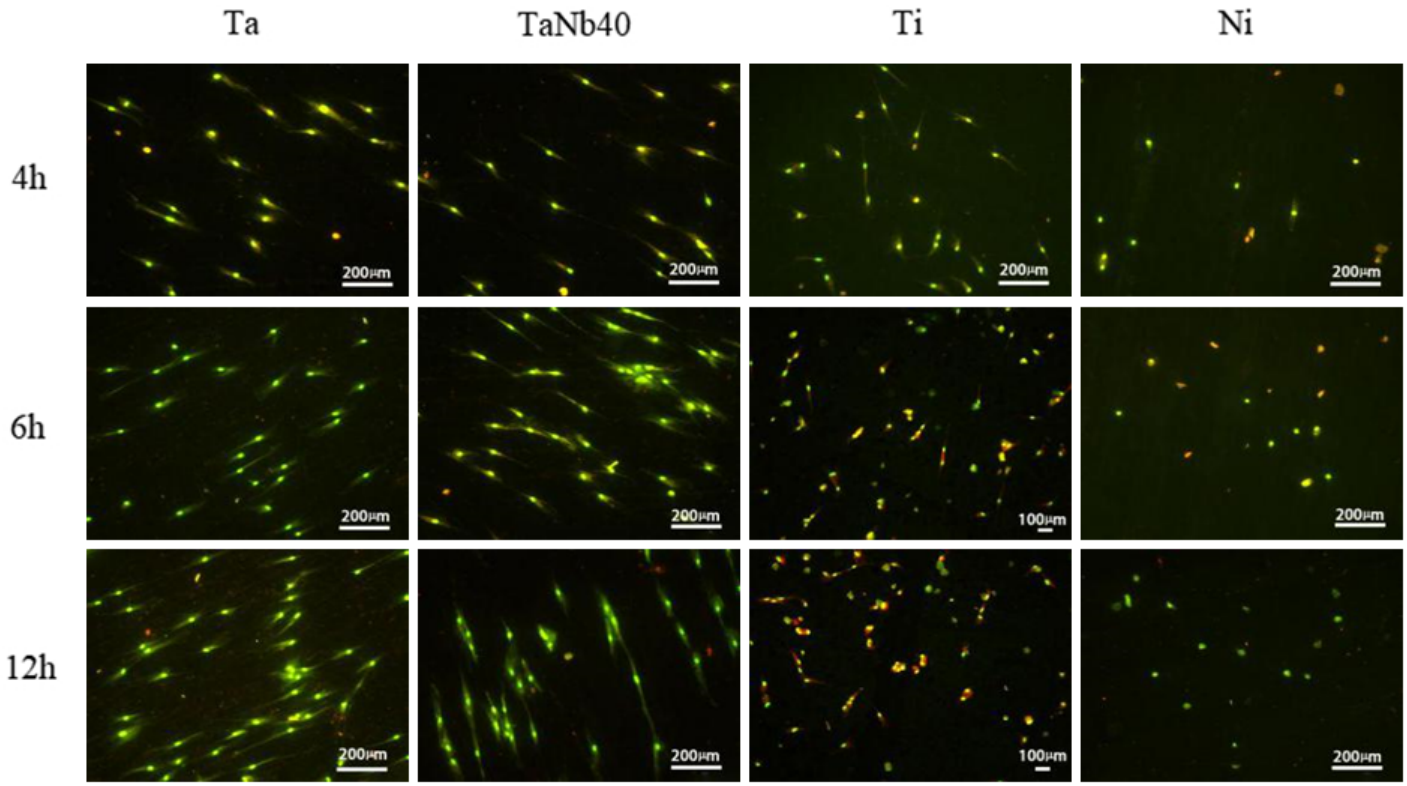

Figure 7

The AO fluorescence micrograph of cells on the different material surface at 4h, 6h, and 12h

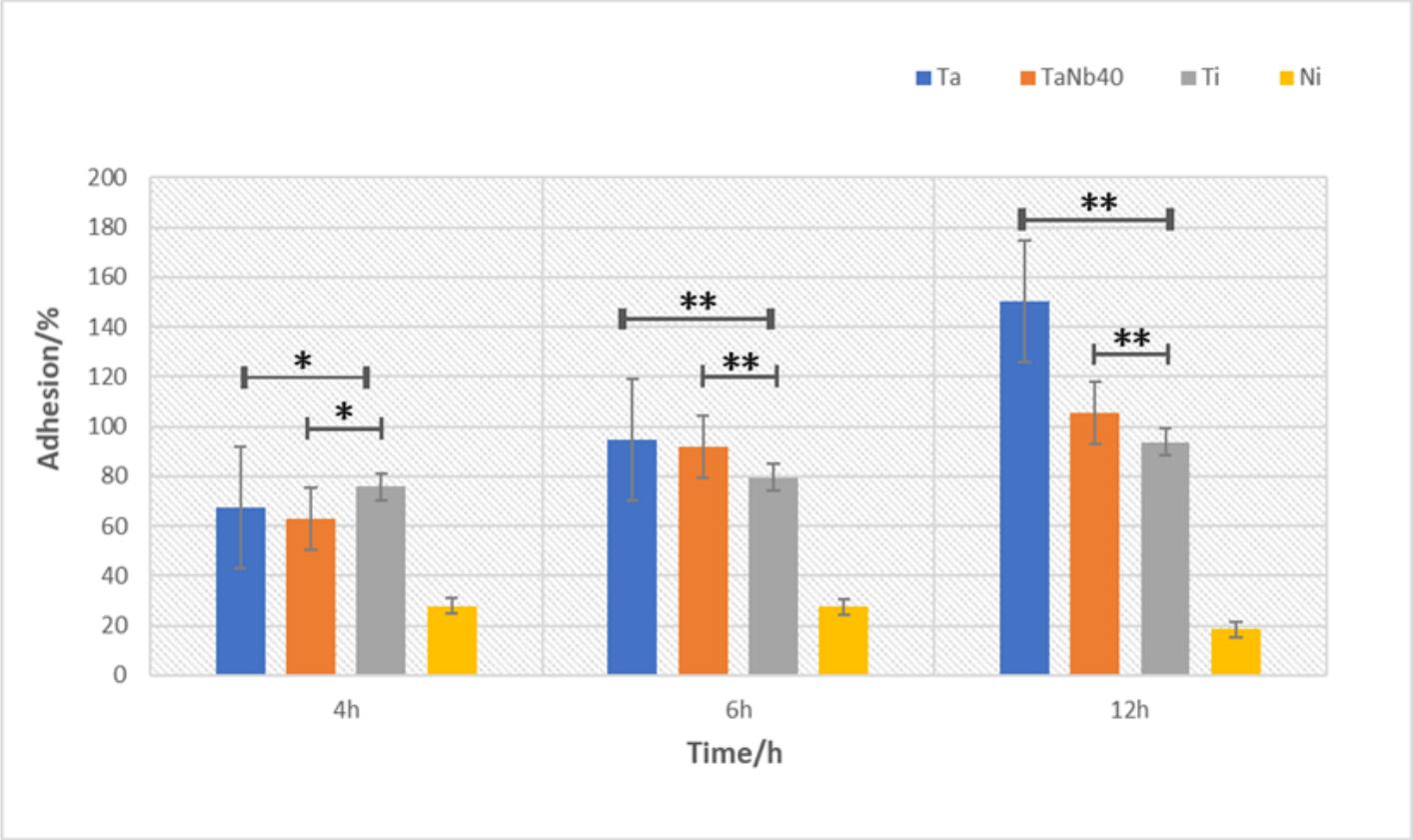

Figure 8

Comparison of the cells early adhesion rate on the different material surtace at 4h, 6h. and 12h (n=5, x ± S, *P<0.05. **P<0.01)

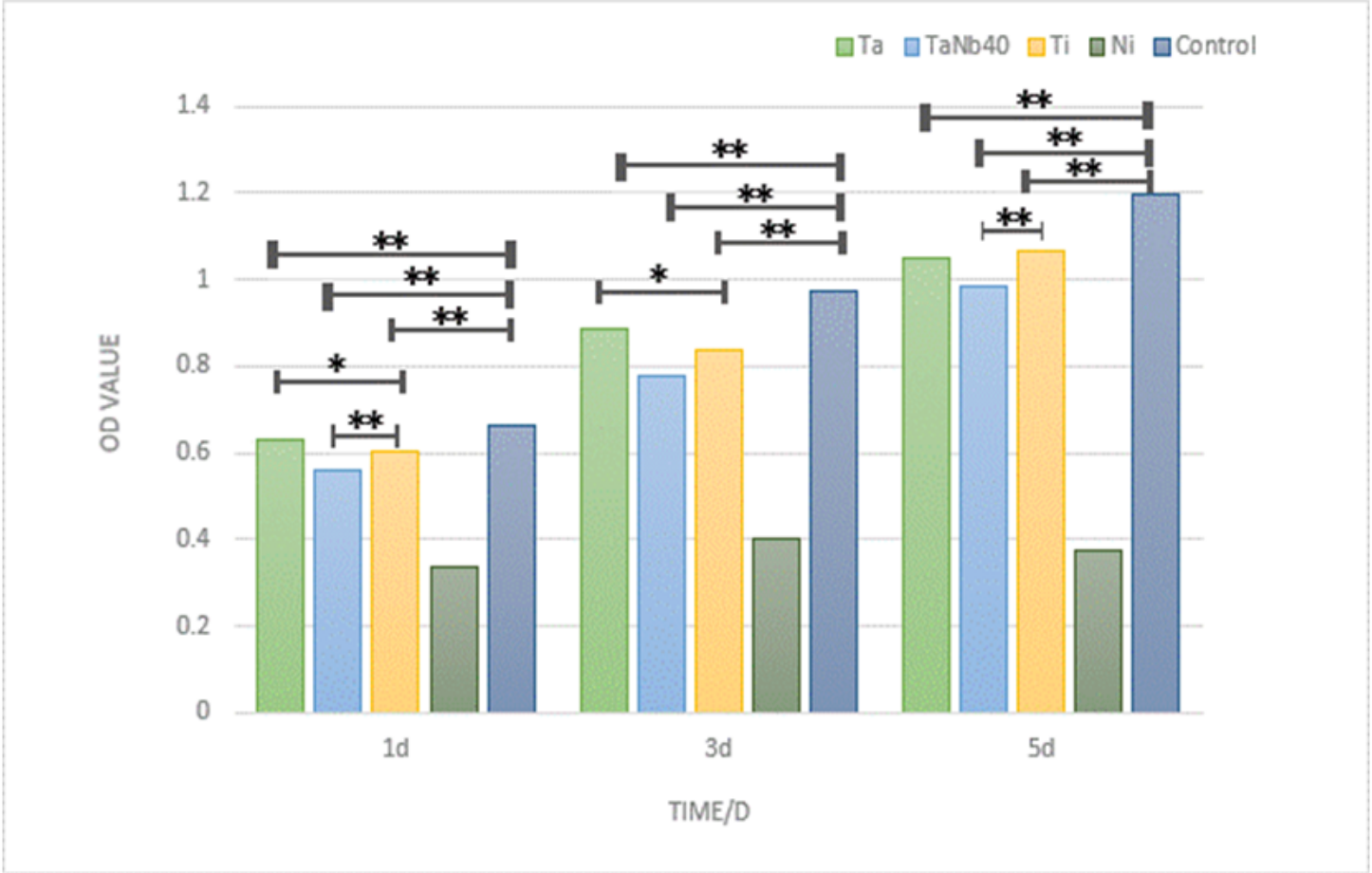

Figure 9

The Comparison of OD value in different extracting liquid for the 1st, 3rd, and 5th day (n=6, x ± S, *P<0.05. **P<0.01)

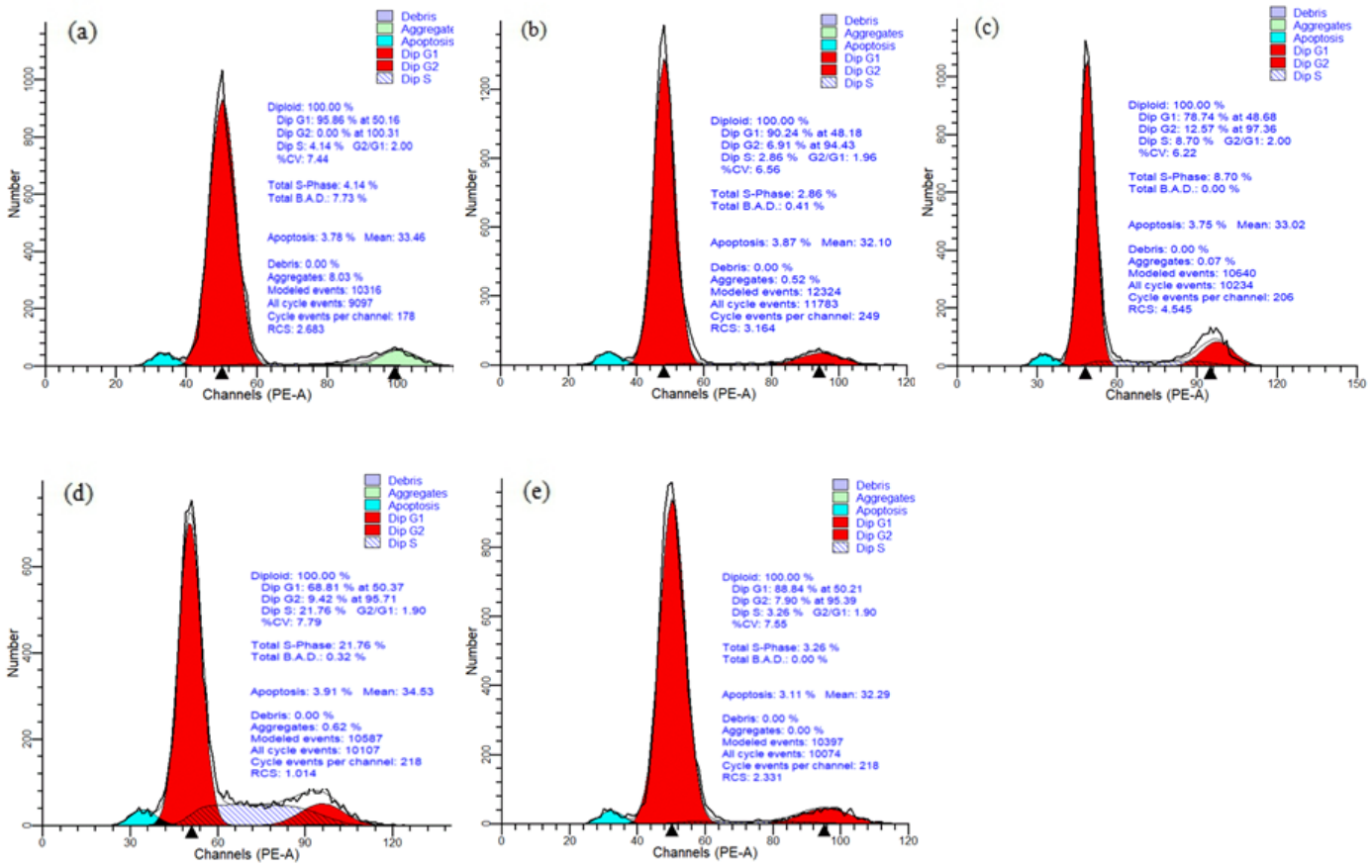

Figure 10

The cells cycle distribution in different extracting liquid after 48h, (a)Ta; (b) TaNo40: (c) Ti; (d) Ni (e) blank control

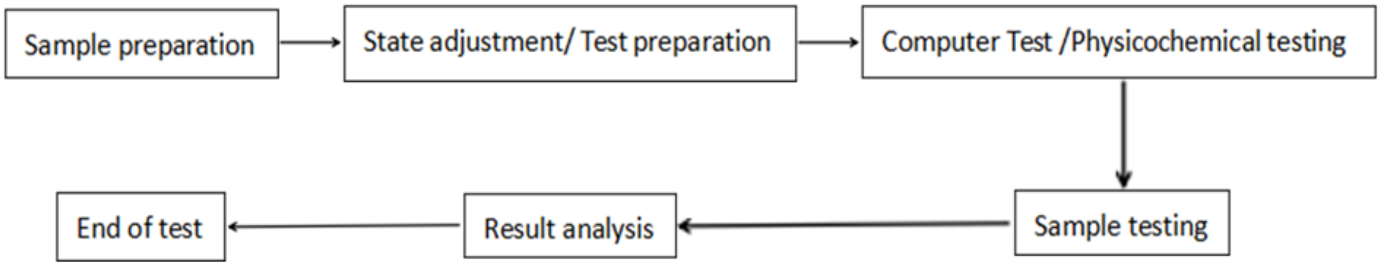

Figure 11

The ICP-MS Gatection process